Electronic Supplementary Information

An amine electrolyte additive with claw structure promoting the stability of a Zn anode in aqueous batteries

Xiaoqi Sun[a,b,*], Hongtu Zhan[a], Qianrui Li[a], Kuo Wang[a,*]

[a.] Department of Chemistry, Northeastern University, Shenyang 110819, China.

[b.] National Frontiers Science Center for Industrial Intelligence and Systems Optimization, Northeastern University, 3-11 Wenhua Road, Shenyang, 110819, China.

*Corresponding authors.

E-mail: sunxiaoqi@mail.neu.edu.cn, 2110043@stu.neu.edu.cn.

1. Experimental Section

1.1 Characterizations

X-ray diffraction (XRD) was measured on a PANalytical Empyrean diffractometer with Cu Kα radiation. The grazing-incidence wide-angle X-ray scattering (GIWAXS) patterns were measured on Bruker D8 (Germany). The morphologies were obtained by a SU8010 scanning electron microscope (HITACHI, Japan). X-ray photoelectron spectroscopy (XPS) was performed on K-Alpha (Thermo Scientific, America). The data was analyzed using CasaXPS software and calibrated by referencing the C 1s peak to 284.8 eV. ^{13}C nuclear magnetic resonance (NMR) was carried out on a Bruker 600 MHz NMR spectrometer (Germany).

1.2 Electrochemical measurements

The electrochemical performance of Zn//Zn, Zn//Cu and Zn//V_2O_5 cells was tested in 2032 coin-type cells. The V_2O_5 cathode was prepared mixing the commercial V_2O_5, Super P and PVDF at a mass ratio of 7:2:1 in N-methyl pyrrolidone (NMP) and drop cast on graphite foil substrate. The active material mass loading was around 1.1 mg cm^{-2}. Cyclic voltammetry (CV) for electrochemical double layer capacitance (EDLC) analysis was performed in Zn//Zn Swagelok® cells. The EDLC values were obtained by the linear fits of *i*-*v* plots according to the equation of $C_{dl} = i/v$. Chronoamperometry (CA) and electrochemical impedance spectroscopy (EIS) measurements were performed in the Zn//Zn symmetric cell. Linear polarization was carried out in three-electrode cells with Zn foil, Cu foil and saturated calomel electrode (SCE) as the working, counter and reference electrodes, respectively. All electrochemical measurements were performed on Bio-logic VMP3 or LANHE CT2001A battery test systems.

1.3 Computational methods

The energy levels of different solvation structures, adsorption energies of different molecules on Zn and corresponding 2D contour map of electron density statistics were

calculated by the DMol3 program package in Materials Studio. The exchange and correlation terms were determined using the Generalized Gradient Approximation (GGA) in the form proposed by Perdew, Burke, and Ernzerhof (PBE). The energy convergence criterion was set to 10^{-6} Hartree. In the Z direction, there was about 15 Å vacuum for erasing the effect of periodic condition for slab model. The adsorbed surfaces of Zn (002) and Zn (100) were constructed with 7*7*3 and 7*5*3 supercells, respectively, corresponding to the dimensions of 18.65*18.65*24.95 $Å^3$ and 18.65*24.73*25.39 $Å^3$. The bottom one layer was kept fixed to maintain bulk properties. For molecular dynamic (MD) simulations, the model was constructed with 3510 H_2O, 126 $ZnSO_4$ and 3 TAA. The COMPASSII force fields were selected for assigning charges for Zn^{2+}, SO_4^{2-}, H_2O and TAA. The geometry optimization was carried out in the Forcite module based on the convergence of total energy (0.001 kcal mol^{-1}) with the force of 0.5 kcal $mol^{-1}Å^{-1}$. MD simulations were then conducted by NVT and NPT ensembles at 298 K. The cutoff distance for van der Waals and electrostatic interactions were 12.5 Å and 12 Å, respectively. All simulations were carried out with the standard periodic boundary condition and the simulation time was long enough to ensure the equilibrium states of electrolyte systems.

2. Supplementary figures and table

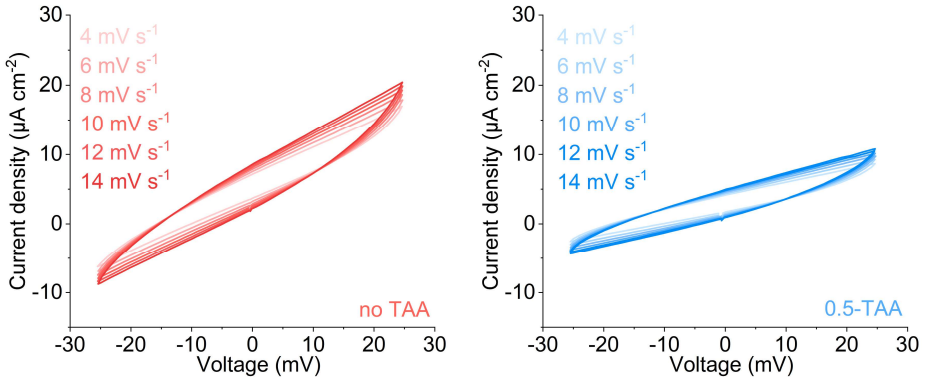

Figure S1. CV curves of Zn symmetric cells in the non-Faradic range in $ZnSO_4$ a) without and b) with 0.5 wt% TAA additive.

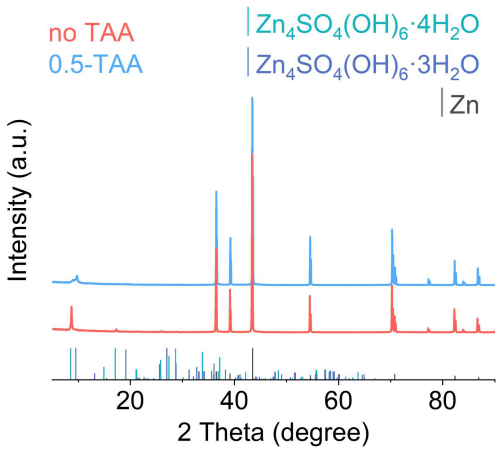

Figure S2. The XRD patterns of Zn soaked in the $ZnSO_4$ solutions without and with 0.5 wt% TAA for 12 h.

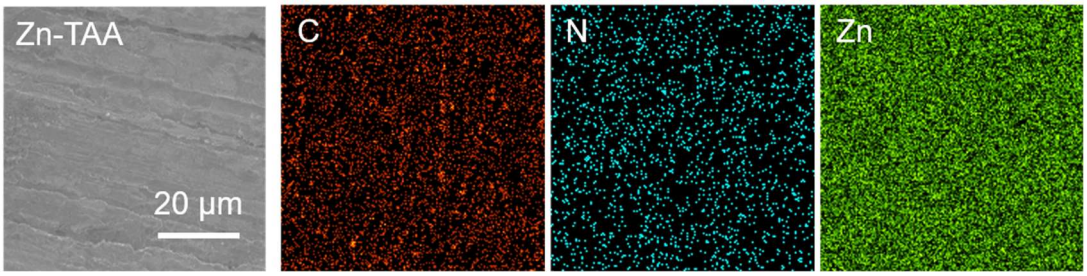

Figure S3. The EDS mappings of Zn soaked in the 0.5 wt% TAA solution for 48 h.

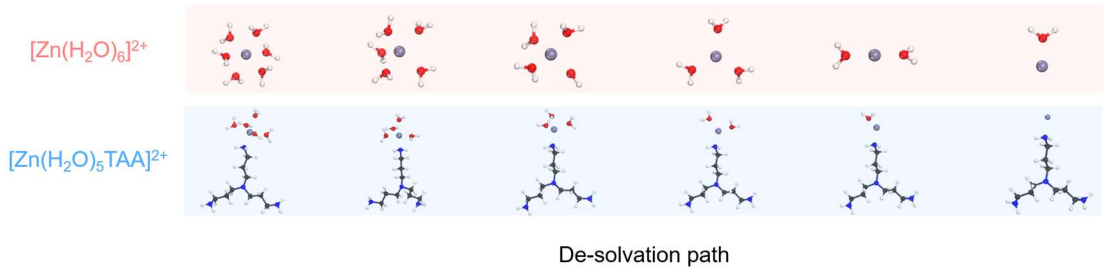

Figure S4. The desolvation configuration at each step of $Zn(H_2O)_6^{2+}$ and $Zn(H_2O)_5TAA^{2+}$ solvation structures.

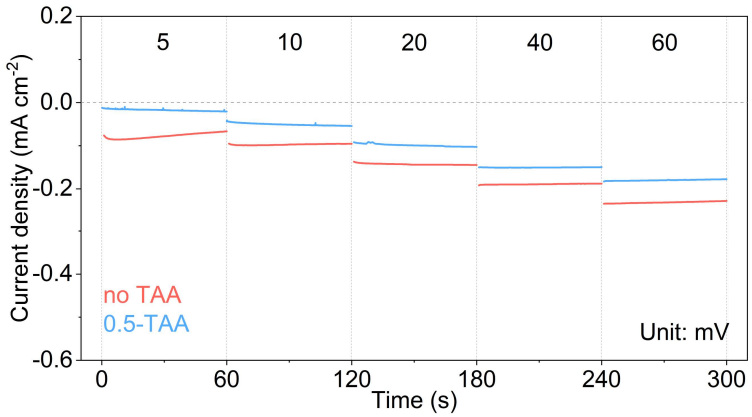

Figure S5. Enlarged CA curves in $ZnSO_4$ without or with 0.5 wt% TAA additive.

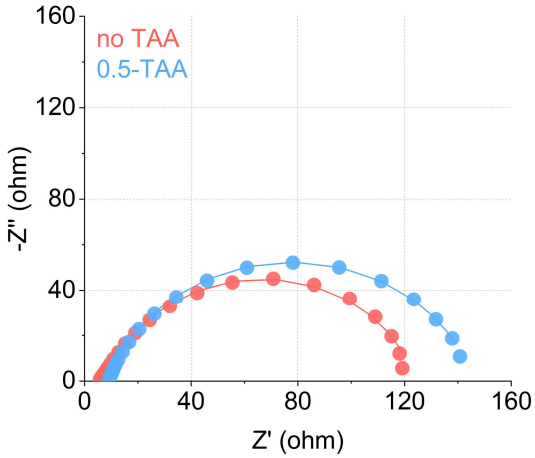

Figure S6. Nyquist plots and fitted curves of Zn electrodes in $ZnSO_4$ without or with 0.5 wt% TAA additive.

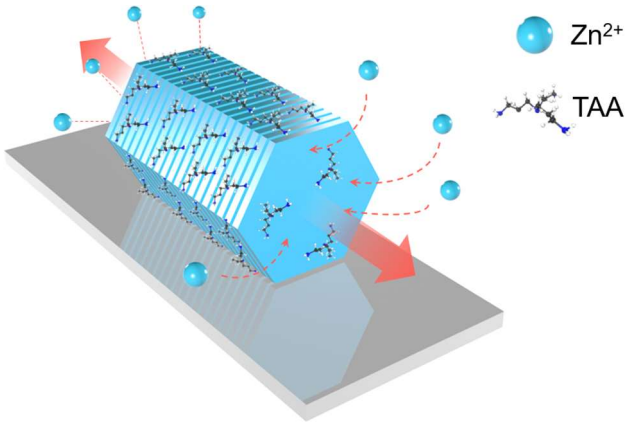

Figure S7. The regulation of Zn deposition orientation by TAA additive.

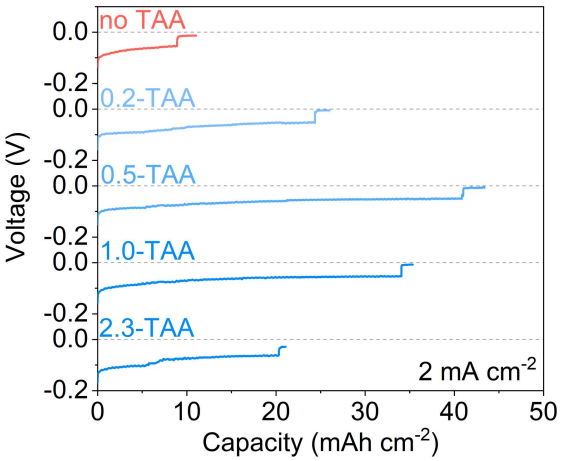

Figure S8. Continuous single plating/stripping voltage curves of Zn symmetric cells in $ZnSO_4$ without and with different percentages of TAA additive.

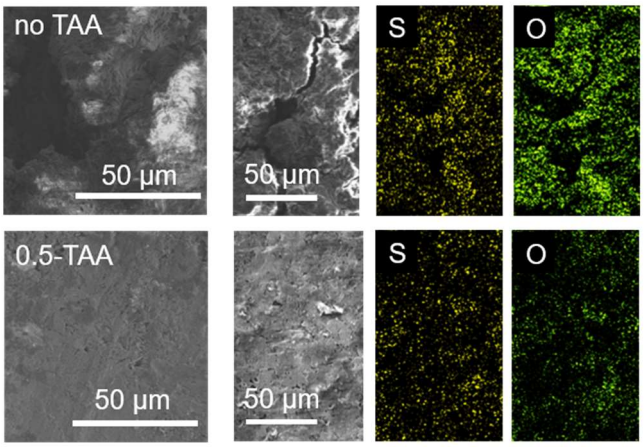

Figure S9. SEM images and EDS mappings of Zn anode cycled from the two electrolytes.

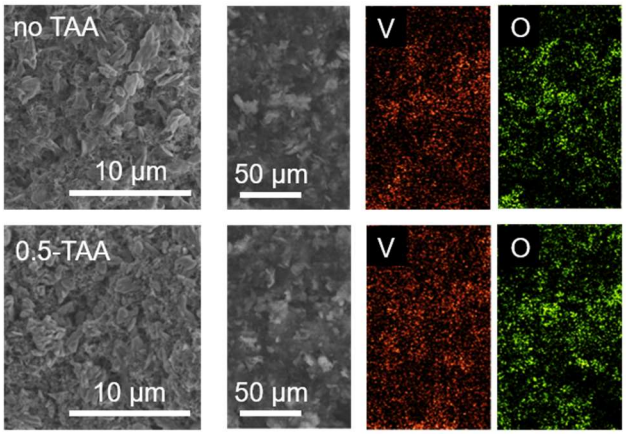

Figure S10. SEM images and EDS mappings of V_2O_5 cathode cycled from the two electrolytes.

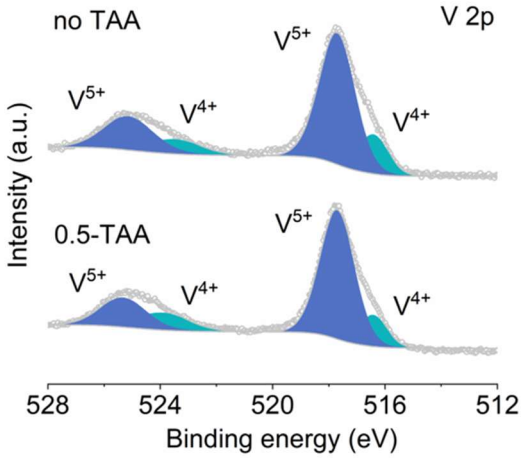

Figure S11. V 2p XPS of V_2O_5 cathode cycled from the two electrolytes.

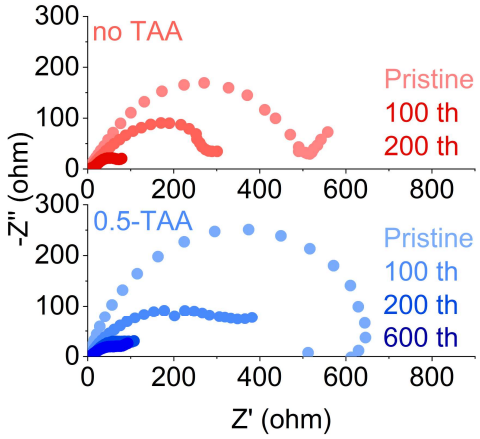

Figure S12. Nyquist plots of Zn//V_2O_5 cells in the baseline $ZnSO_4$ and 0.5-TAA electrolytes at different cycles.

Table S1. The cycling performance of Zn//V_2O_5 battery using the 0.5-TAA electrolyte in comparison to previous studies.

Electrolyte additive or artificial layer on Zn	Current density (A g^{-1})	Cycle number	Capacity retained (mAh g^{-1})	Ref.
NFSS@Zn-MnO_2	3	1000	115.7	1
TXA additive-NiCo-MnO_2	3	1000	92.5	2
TAU additive-$NH_4V_4O_{10}$	3	1000	117	3
CTAB additive-MnO_2	4	1000	126.56	4
Gln additive-$NH_4V_4O_{10}$	5	800	90.3	5
	10	800	58.3	
Zn@H-SPEEK-NMO	5	1000	66.57	6
TAA additive-V_2O_5	5	1000	185	This work

3. References

[1] C. Huang, X. Zhao, Y. Hao, Y. Yang, Y. Qian, G. Chang, Y. Zhang, Q. Tang, A. Hu and X. Chen, Self-Healing SeO2 Additives Enable Zinc Metal Reversibility in Aqueous ZnSO4 Electrolytes, *Advanced Functional Materials*, 2022, **32**, 2112091.

[2] J. Yin, H. Liu, P. Li, X. Feng, M. Wang, C. Huang, M. Li, Y. Su, B. Xiao, Y. Cheng and X. Xu, Integrated electrolyte regulation strategy: Trace trifunctional tranexamic acid additive for highly reversible Zn metal anode and stable aqueous zinc ion battery, *Energy Storage Materials*, 2023, **59**, 102800.

[3] X. Xu, J. Yin, R. Qin, H. Liu, X. Feng, M. Wang, M. Li, W. Sun, W. Shi, B. Xiao, Y. Su and Y. Cheng, Simultaneous regulation on coordination environment and interfacial chemistry via taurine for stabilized Zn metal anode, *Journal of Energy Chemistry*, 2023, **86**, 343-350.

[4] Z. Liu, R. Wang, Y. Gao, S. Zhang, J. Wan, J. Mao, L. Zhang, H. Li, J. Hao, G. Li, L. Zhang and C. Zhang, Low-Cost Multi-Function Electrolyte Additive Enabling Highly Stable Interfacial Chemical Environment for Highly Reversible Aqueous Zinc Ion Batteries, *Advanced Functional Materials*, 2023, **33**, 2308463.

[5] J. Yin, M. Li, X. Feng, T. Cui, J. Chen, F. Li, M. Wang, Y. Cheng, S. Ding, X. Xu and J. Wang, Unveiling the multifunctional regulation effect of a glutamine additive for highly reversible Zn metal anodes, *Journal of Materials Chemistry A*, 2024, **12**, 1543-1550.

[6] J. Wang, Y. Yu, R. Chen, H. Yang, W. Zhang, Y. Miao, T. Liu, J. Huang and G. He, Induced Anionic Functional Group Orientation-Assisted Stable Electrode-Electrolyte Interphases for Highly Reversible Zinc Anodes, *Advanced Science*, 2024, **11**, 2402821.